

# $\gamma$ -Synucleinopathy: neurodegeneration associated with overexpression of the mouse protein

Natalia Ninkina<sup>1</sup>, Owen Peters<sup>1</sup>, Steven Millership<sup>1</sup>, Hatem Salem<sup>1</sup>, Herman van der Putten<sup>2</sup> and Vladimir L. Buchman<sup>1,\*</sup>

<sup>1</sup>School of Biosciences, Cardiff University, Museum Avenue, Cardiff CF10 3AX, UK and <sup>2</sup>Neuroscience, Novartis Institutes for Biomedical Research, Novartis AG CH-4002, Basel, Switzerland

Received January 8, 2009; Revised February 12, 2009; Accepted February 20, 2009

The role of  $\alpha$ -synuclein in pathogenesis of familial and idiopathic forms of Parkinson's disease, and other human disorders known as  $\alpha$ -synucleinopathies, is well established. In contrast, the involvement of two other members of the synuclein family,  $\beta$ -synuclein and  $\gamma$ -synuclein, in the development and progression of neurodegeneration is poorly studied. However, there is a growing body of evidence that  $\alpha$ -synuclein and  $\beta$ -synuclein have opposite neuropathophysiological effects. Unlike  $\alpha$ -synuclein, overexpressed  $\beta$ -synuclein does not cause pathological changes in the nervous system of transgenic mice and even ameliorates the pathology caused by overexpressed  $\alpha$ -synuclein. To assess the consequences of excess expression of the third family member,  $\gamma$ -synuclein, on the nervous system we generated transgenic mice expressing high levels of mouse  $\gamma$ -synuclein under control of Thy-1 promoter. These animals develop severe age- and transgene dose-dependent neuropathology, motor deficits and die prematurely. Histopathological changes include aggregation of  $\gamma$ -synuclein, accumulation of various inclusions in neuronal cell bodies and processes, and astrogliosis. These changes are seen throughout the nervous system but are most prominent in the spinal cord where they lead to loss of spinal motor neurons. Our data suggest that down-regulation of small heat shock protein HSPB1 and disintegration of neurofilament network play a role in motor neurons dysfunction and death. These findings demonstrate that  $\gamma$ -synuclein can be involved in neuropathophysiological changes and the death of susceptible neurons suggesting the necessity of further investigations of the potential role of this synuclein in disease.

## INTRODUCTION

The importance of  $\alpha$ -synuclein in the development and progression of the human disorders known as synucleinopathies is beyond doubt although the exact mechanism of neurodegeneration induced by dysfunction of this protein is the subject of heated debate [for recent reviews see Ref. (1)]. On the other hand,  $\beta$ -synuclein is believed to be a neuroprotective factor—in several experimental *in vivo* systems, expression of this protein ameliorated neuronal pathology caused by overexpression of  $\alpha$ -synuclein (2–7).

Despite limited information, certain known properties of  $\gamma$ -synuclein place it structurally and functionally in between the other two members of the synuclein family. For instance,

$\gamma$ -synuclein adopts a free-state residual secondary structure similar to  $\alpha$ -synuclein whereas in an extended mode its structure resembles  $\beta$ -synuclein (8). These structural differences correlate with different propensities of the synucleins to aggregate. Aggregation of  $\alpha$ -synuclein *in vivo* is believed to be a crucial event in pathogenesis of these diseases, with intermediates (i.e. soluble oligomers) and final products (i.e. larger, insoluble and immunohistochemically detectable aggregates) playing different but equally important roles (1,9,10). Conversely, a protective function of  $\beta$ -synuclein seems to correlate with its negligible propensity to aggregate and its ability to retard the aggregation of  $\alpha$ -synuclein *in vitro* (2,11–13).  $\gamma$ -Synuclein is able, albeit less efficiently than  $\alpha$ -synuclein, to aggregate and form fibrils *in vitro*. However, like

\*To whom correspondence should be addressed at: Cardiff University, Museum Avenue, Cardiff, CF10 3AX, UK. Tel: +44 2920879068; Fax: +44 2920874116; Email: buchmanvl@cardiff.ac.uk

$\beta$ -synuclein, it has also been shown to inhibit the aggregation of  $\alpha$ -synuclein (11,12). In contrast to  $\alpha$ -synuclein, acute overexpression of  $\gamma$ -synuclein does not induce death of cultured neurons but perturbs their neurofilament network by an unknown mechanism (14,15).

While  $\alpha$ -synuclein is the major component of Lewy bodies and other histopathological hallmarks of synucleinopathies, neither  $\beta$ -synuclein nor  $\gamma$ -synuclein have been found in these structures. Nonetheless, changes in their expression or distribution (16–18) and accumulation of these proteins in unconventional histopathological lesions within neurons and axons (Refs 19–21 and our unpublished observations) have been observed in several human neurodegenerative disorders as well as certain transgenic or pharmacological animal models of neurodegeneration (16,22–26). Therefore, it is tempting to speculate that accumulation and aggregation of  $\gamma$ -synuclein might be a causative factor in the development of certain, yet to be identified, types of neurological disorders.

To test whether increased and/or ectopic expression of mouse  $\gamma$ -synuclein could trigger neurohistopathological changes and phenotypes typical for synucleinopathies, we produced transgenic mice with pan-neuronal overexpression of this protein. Animals expressing high levels of  $\gamma$ -synuclein develop severe and fatal neurological disease associated with aggregation of the overexpressed protein and its deposition in cytoplasmic and axonal lesions.

## RESULTS

### Production of transgenic animals and analysis of transgene expression

Transgenic mice expressing elevated levels of mouse wild-type  $\gamma$ -synuclein were generated using the Thy-1 neuron-specific expression cassette (Fig. 1A) that we and others have used previously for generating lines expressing high levels of either  $\alpha$ -synuclein (27–30) or  $\beta$ -synuclein (5). Mice from one line, Thy1m $\gamma$ SN, expressed high levels of mouse  $\gamma$ -synuclein throughout the nervous system and developed an age-dependent neurological phenotype. Mice of a second line with lower levels of the transgene expression did not develop a noticeable phenotype and were excluded from this study.

Transgenic mice were produced on a pure genetic background and the colony was maintained by backcrossing hemizygous Thy1m $\gamma$ SN mice with C57Bl6 mice. These hemizygous animals were indistinguishable from their wild-type littermates during the first year of their life. Later most of these mice developed a clasping reflex, abnormal posture and gait, as well as other signs of motor dysfunction (see below). In an attempt to augment the pathology we bred Thy1m $\gamma$ SN mice to homozygosity. This resulted in an approximate doubling of the transgene expression levels, which in dorsal root ganglia (DRG) of 12-month-old mice reached the level that was approximately seven times higher than the level of endogenous  $\gamma$ -synuclein mRNA in these ganglia (Fig. 1B). Offspring from intercrosses of hemizygous parents showed a normal Mendelian distribution of genotypes. Homozygous animals appeared normal during the first few months of life despite a very high level of  $\gamma$ -synuclein

mRNA expression throughout their nervous system. For instance, in the spinal cord of young adult homozygous transgenic animals, the level of this mRNA was approximately 16 times higher than in the trigeminal ganglion of wild-type mice that was used for reference due to the high endogenous level of  $\gamma$ -synuclein mRNA expression and homogeneity of cell population in this structure (Fig. 1B, top panel). In the spinal cord of wild-type animals, only motor neurons express  $\gamma$ -synuclein (31), but in Thy1m $\gamma$ SN mice, motorneurons and additional types of spinal neurons expressed  $\gamma$ -synuclein, which explains, in part, the robust increase of both  $\gamma$ -synuclein mRNA (Fig. 1B, bottom panel) and protein (Fig. 1C and D) levels. The same applied to other regions (Fig. 1D and data not shown) where endogenous  $\gamma$ -synuclein expression is restricted to certain neuronal populations (32) but the transgene is expressed in the majority of neurons. Substantial accumulation of  $\gamma$ -synuclein did not affect the levels of expression of the other two members of synuclein family (Fig. 1D).

### Overexpression of $\gamma$ -synuclein is associated with a severe neurological phenotype and early lethality of transgenic mice

The health of homozygous animals started to deteriorate substantially from the age of 6–9 months. The first signs of pathology were similar to those observed in the older hemizygous mice, including clasping reflex, hunchback posture and abnormal gait (Fig. 2A–C and Supplementary Material movie). In contrast to hemizygous animals, clinical signs of pathology in homozygous animals progressed rapidly with all animals developing pareses of their limbs by the age of 9–16 months followed by paralyses and loss of the righting reflex (Fig. 2D). At this stage, the animals were sacrificed to prevent further suffering. Typically, the paraparesis of the forelimbs became obvious earlier than that of the hindlimbs. Lifespan of homozygous transgenic mice was also limited; not a single mouse survived beyond the age of 16 months in two independent cohorts (total 74 mice) housed in two animal facilities (Fig. 2E).

The onset and progression of motor dysfunction was quantified using several different tests. Balance and coordination were already significantly impeded in homozygous Thy1m $\gamma$ SN mice younger than 6 months before they displayed obvious clinical signs of pathology (Fig. 3 and Supplementary Material Tables S1 and S2). Their ability to turn on an 11 mm diameter beam and their performance on a constant speed rotarod were both compromised by the age of 4 months (Fig. 3A and Supplementary Material Table S1). Using the accelerating rotarod test, it was possible to demonstrate motor impairments as early as at 2 months of age. At this time point the homozygous Thy1m $\gamma$ SN mice were indistinguishable from wild-type mice by any other criteria examined (Fig. 3B). Hemizygous Thy1m $\gamma$ SN mice developed a similar motor dysfunction but with a much greater latency and slower progression. This is exemplified by their performance on the rotarod that only declined significantly after the age of 18 months (Fig. 3). In the footprint test, the length of stride of hemizygous 18-month-old animals was significantly shorter than that of their wild-type littermates, while

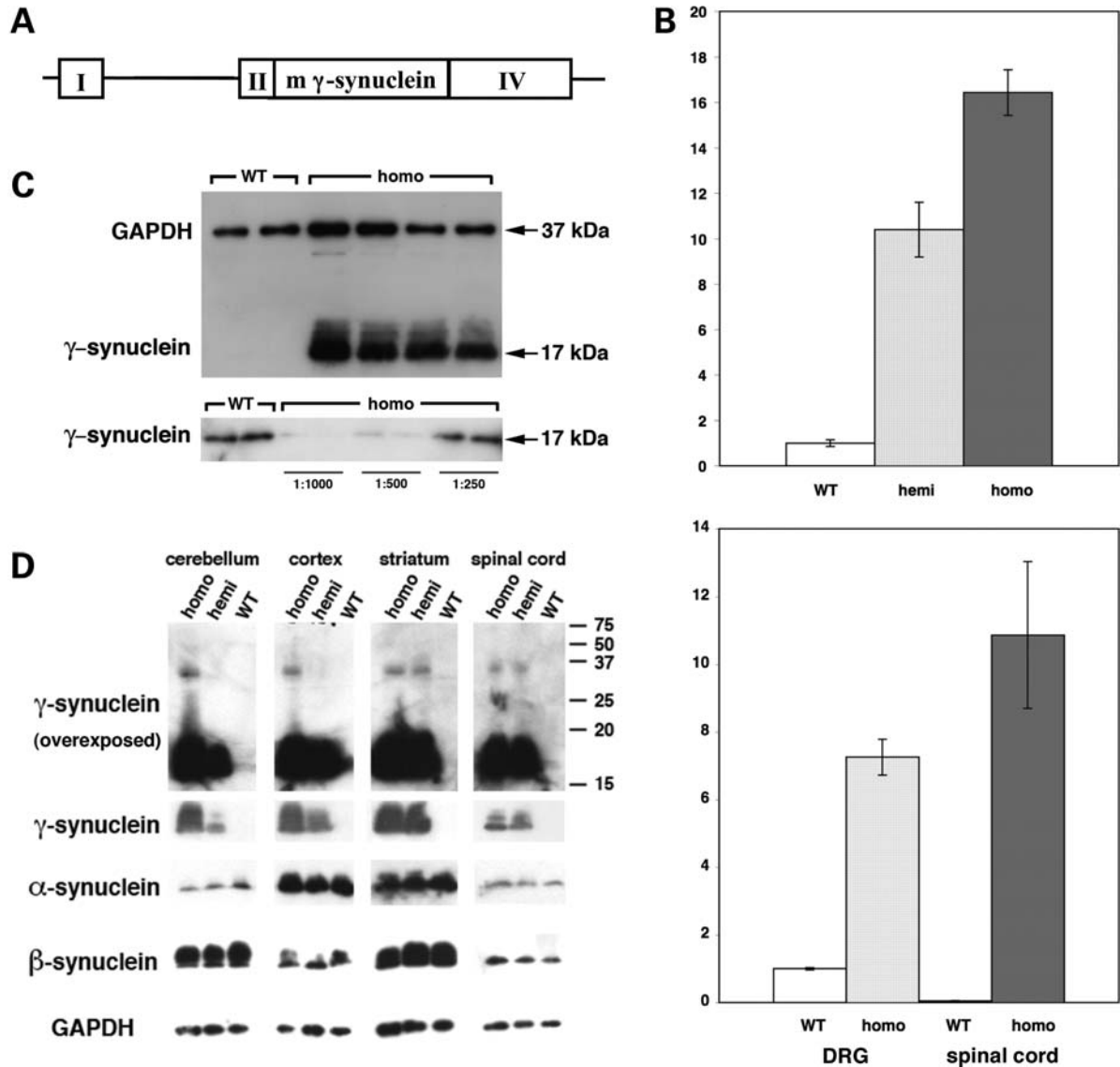


**Figure 1.** Expression of  $\gamma$ -synuclein in wild-type and transgenic mice. (A) A map of DNA fragment used for producing transgenic animals. A mouse  $\gamma$ -synuclein cDNA fragment was inserted between exons II and IV of the mouse Thy-1 gene. (B) Expression of  $\gamma$ -synuclein mRNA in neuronal tissues of wild-type and transgenic animals measured by quantitative real-time RT-PCR. Bar charts show the fold  $\gamma$ -synuclein mRNA level increase (mean  $\pm$  SEM) in the spinal cord of homozygous and heterozygous 8-week-old Thy1m $\gamma$ SN mice compared with the level in the trigeminal ganglion of newborn wild-type mice (top chart) and in the DRG and spinal cord of homozygous 12-month-old Thy1m $\gamma$ SN mice compared with the level in the DRG of 12-month-old wild-type mice (bottom chart). (C) Western blot analysis of  $\gamma$ -synuclein in the spinal cord of 1-year-old wild-type and homozygous Thy1m $\gamma$ SN animals. The top panel shows a normalization western blot simultaneously probed with antibodies against GAPDH and  $\gamma$ -synuclein. The same undiluted wild-type samples and 1:1000, 1:500 or 1:250 diluted transgenic samples were analysed on a western blot shown in the bottom panel. (D) Western blot analysis of three synucleins in neuronal tissues of homozygous than hemizygous mice but a ladder of multimeric  $\gamma$ -synuclein-positive bands is not observed even on overexposed western blots (top panels).

homozygous mice already showed this impairment at the age of 6 months (Supplementary Material Fig. S1 and data not shown). The horizontal beam test was most sensitive for detecting early signs of motor deficit in hemizygous Thy1m $\gamma$ SN animals; their ability to perform both parts of the task was already obviously compromised at the age of 12 months (Supplementary Material Tables 1 and 2).

In summary, pan-neuronal overexpression of mouse  $\gamma$ -synuclein in transgenic mice was associated with a progressive age- and gene dose-dependent motor phenotype that recapitulates

phenotypes described earlier for several lines expressing human  $\alpha$ -synuclein under control of the same Thy-1 promoter or other pan-neuronal promoters (27,30,33–39).

#### Aggregation and fibrillation of $\gamma$ -synuclein in the nervous system of transgenic mice

It was feasible to suggest that pathological changes in the nervous system of Thy1m $\gamma$ SN transgenic mice would also be similar to the changes observed in the nervous system of

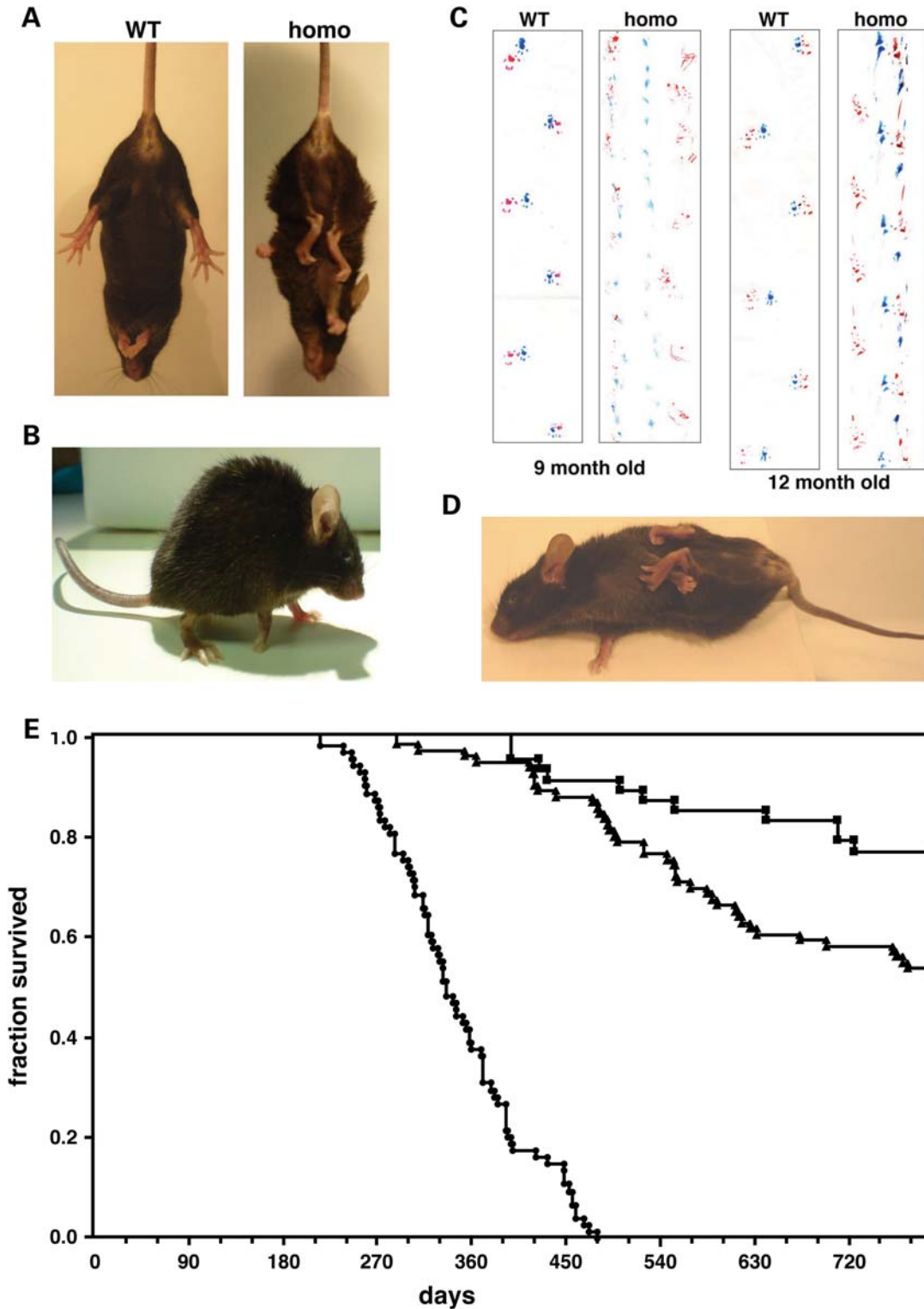


**Figure 2.** Transgenic animals develop pathology that leads to premature death. Typical appearance of Thy1m $\gamma$ SN transgenic mice at the initial stage of pathology development with claspings of all limbs when hanging by the tail (**A**) and a hunchback posture (**B**). Examples of severe gait abnormality in 9- and 12-month-old homozygous  $\gamma$ -synuclein transgenic mice detected by the footprint test. Forefeet prints are blue and hindfeet prints are red (**C**). At the advanced stage of pathology, the righting reflex is substantially impaired (**D**). Kaplan–Meier plot of wild-type (squares,  $n = 49$ ), hemizygous Thy1m $\gamma$ SN (triangles,  $n = 87$ ) and homozygous Thy1m $\gamma$ SN (circles,  $n = 74$ ) mice survival over the 26 months period (**E**).

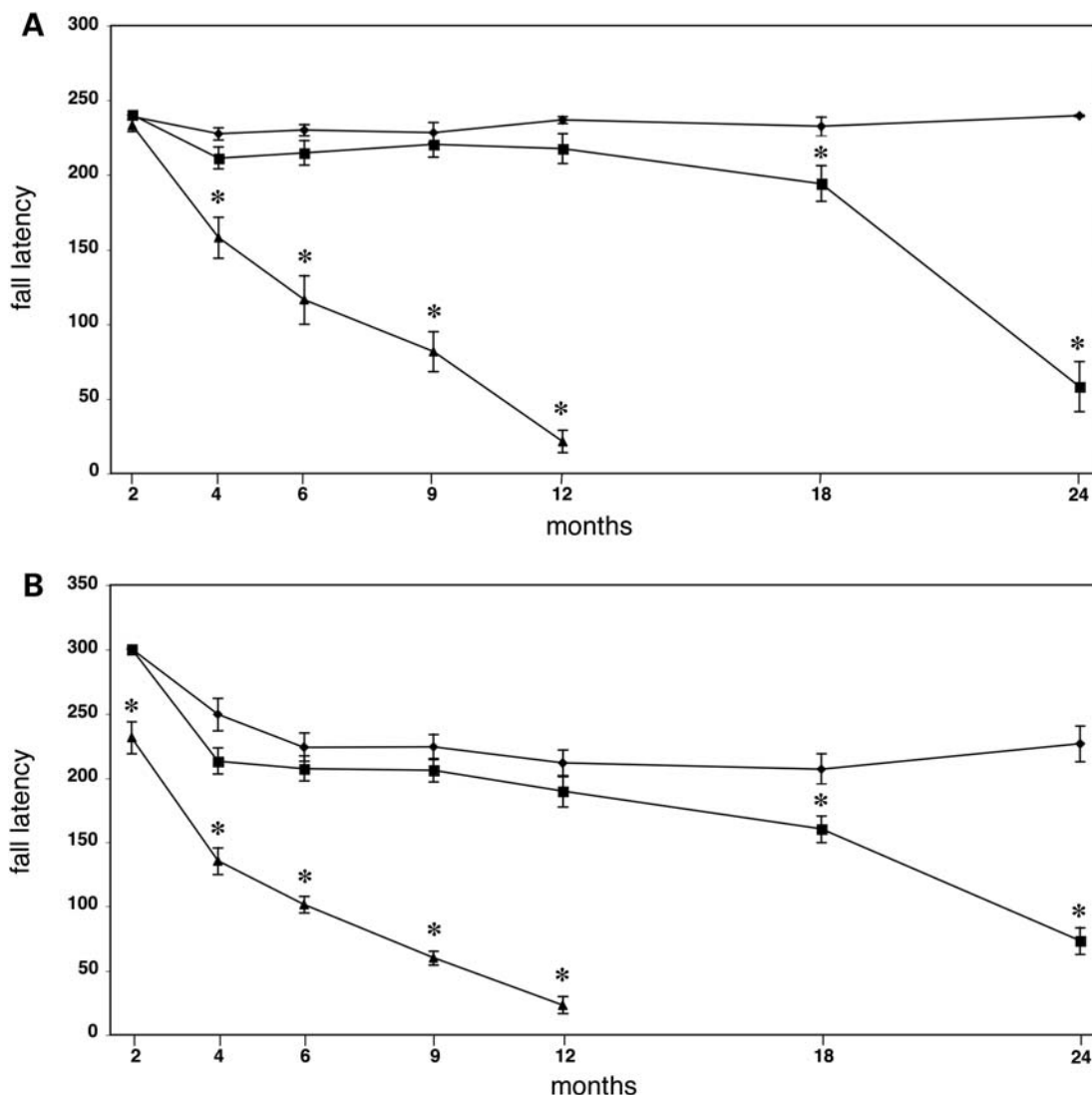


**Figure 3.** Rotarod performance of  $\gamma$ -synuclein transgenic mice. Groups of mice of different ages and genotypes were tested on Ugo Basile rotarod using constant speed (A) or accelerating (B) modes as described in Material and methods. Line graphs show mean  $\pm$  SEM of latency to fall for wild-type (diamonds), hemizygous Thy1m $\gamma$ SN (squares) and homozygous (triangles) Thy1m $\gamma$ SN mice at different age. Statistically significant difference ( $P < 0.01$ , Student's  $t$ -test) in performance between transgenic and wild type groups at particular age is denoted by asterisks.

$\alpha$ -synuclein transgenic animals and might be accompanied by aggregation of  $\gamma$ -synuclein in neurons and their processes. Therefore, we looked for signs of  $\gamma$ -synuclein aggregation throughout the nervous system of homozygous Thy1m $\gamma$ SN mice that developed obvious pathology.

Immunohistochemical analysis of Thy1m $\gamma$ SN brain and spinal cord sections stained with highly specific SK23 antibody (31) revealed increased production of  $\gamma$ -synuclein in many neurons expressing endogenous  $\gamma$ -synuclein as well as ectopic production in other neurons normally devoid of this protein. In contrast to the predominantly neuritic localization of endogenous  $\gamma$ -synuclein in the brain of adult wild-type mice (32), overproduced protein also accumulated in the neuronal cell bodies (Supplementary Material Fig. S2). Although immunostaining in the majority of transgenic mouse brain neurons was diffusely distributed throughout the cytoplasm, in subsets of neurons, we detected  $\gamma$ -synuclein-positive

cytoplasmic inclusions which, in some cases, were clearly eosinophilic and also showed some remarkable resemblance to the  $\alpha$ -synuclein-positive structures seen in Lewy body diseases (Fig. 4A and Supplementary Material Fig. S2D and E). However, much more typical was the presence of  $\gamma$ -synuclein-positive spheroids and dystrophic neurites (Fig. 4A and Supplementary Material Fig. 2D and E) that were not seen in the nervous system of wild-type littermates (Fig. 4A and data not shown).

These abnormal structures were observed throughout the nervous system but were most abundant in the spinal cord (Fig. 4A), which is consistent with the observed clinical pattern of pathology. Therefore, the spinal cord was used to determine whether aggregated and fibrillated forms of  $\gamma$ -synuclein were present in neuronal tissues of animals over-expressing this protein. Sequential fractionation of the spinal cord tissues demonstrated that, in contrast to endogenous

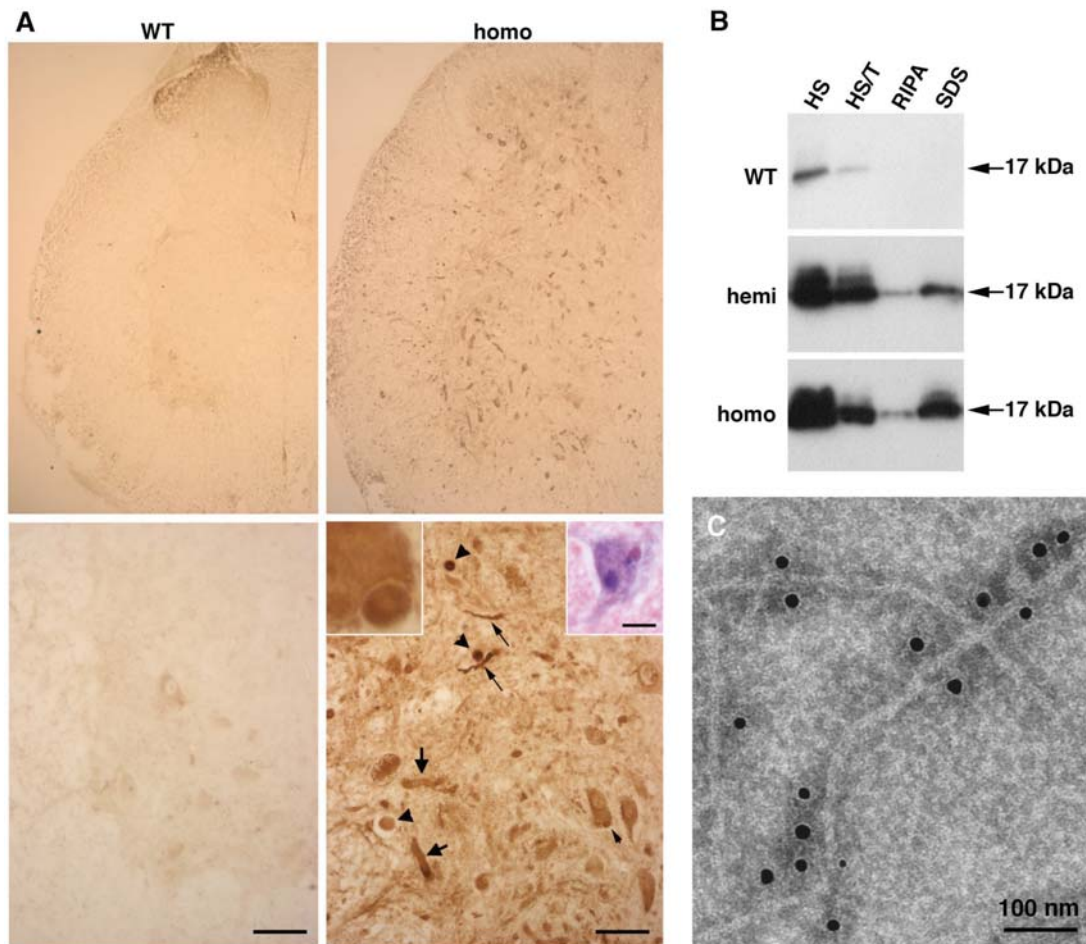


**Figure 4.**  $\gamma$ -Synuclein-positive aggregates and fibrils in the spinal cord of 12-month-old transgenic mice detected by anti-mouse  $\gamma$ -synuclein SK23 antibody. (A) Immunostained transverse sections through the spinal cord of wild-type and homozygous  $\gamma$ -synuclein transgenic mice. Higher magnification images of the ventral horn region are shown on lower panels, scale bars = 50  $\mu$ m. A  $\gamma$ -synuclein-positive cytoplasmic inclusion (further magnified in the left inset) is indicated by the small arrowheads, spheroids by large arrowheads, dystrophic and ballooned neurites by small and large arrows, correspondingly. The right inset shows a hematoxylin and eosin-stained spinal cord motor neuron with an eosinophilic cytoplasmic inclusion, scale bar = 20  $\mu$ m. (B) Western blot analysis of  $\gamma$ -synuclein in high salt (HS), HS/Triton X-100 (HS/T), RIPA- and SDS-soluble fractions of the spinal cord of wild-type, hemizygous and homozygous mice. (C) Immuno-electron microscopy detection of  $\gamma$ -synuclein fibrils in a sarcosyl-insoluble fraction of the homozygous Thy1m $\gamma$ SN mouse spinal cord.

$\gamma$ -synuclein, which was completely soluble in salt/non-ionic detergent buffers, a substantial fraction of  $\gamma$ -synuclein in the spinal cord of Thy1m $\gamma$ SN mice remained insoluble after extraction with these solutions but could be partially solubilized in the ionic detergent-containing buffers (Fig. 4B) or in formic acid (data not shown). Immuno-electron microscopy of sarcosyl-insoluble material revealed the presence of filaments decorated with antibody against  $\gamma$ -synuclein (Fig. 4C). These results demonstrate that increased expression of  $\gamma$ -synuclein in mouse neurons can cause aggregation and fibrillation of this protein followed by formation of large intracellular inclusions.

#### Histopathology in the spinal cord of transgenic mice

Amyloid-like inclusions were detected by Congo Red (Fig. 5B–D) or thioflavine S (data not shown) staining of spinal cord or brain tissue of hemi- and homozygous mice, even at a stage when clinical signs of pathology were mild

(only clasp reflex). The number of the Congo Red-positive inclusions substantially increased as disease progressed (Fig. 5E).

Neuronal degeneration is commonly associated with the activation of microglia and astroglia in affected regions of the nervous system. A large number of GFAP-positive cells with morphology typical for activated astrocytes were found in the spinal cord gray matter of severely affected homozygous Thy1m $\gamma$ SN mice (Fig. 6A). The level of GFAP was also substantially increased in the spinal cord tissue of homozygous and, to a lesser extent, age-matched hemizygous animals without obvious signs of pathology (Fig. 6B) but not in the spinal cord of young homozygous mice. However, using antibodies against two different markers, Iba1 and CD11b, we failed to detect clear signs of microglia activation (data not shown).

Another common feature of synucleinopathies is the presence of ubiquitin-positive inclusions in affected regions of the nervous system. In the spinal cord of  $\gamma$ -synuclein

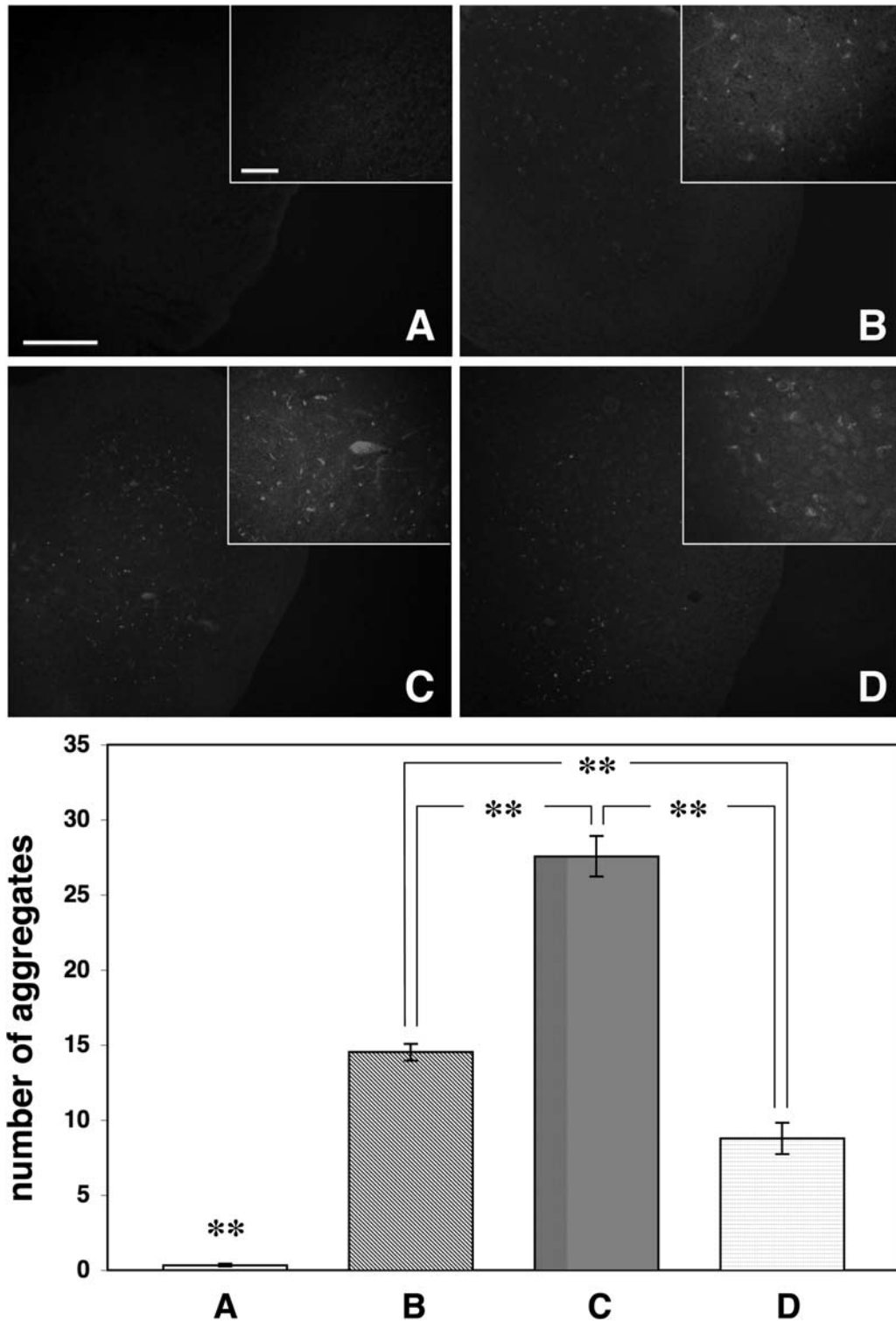
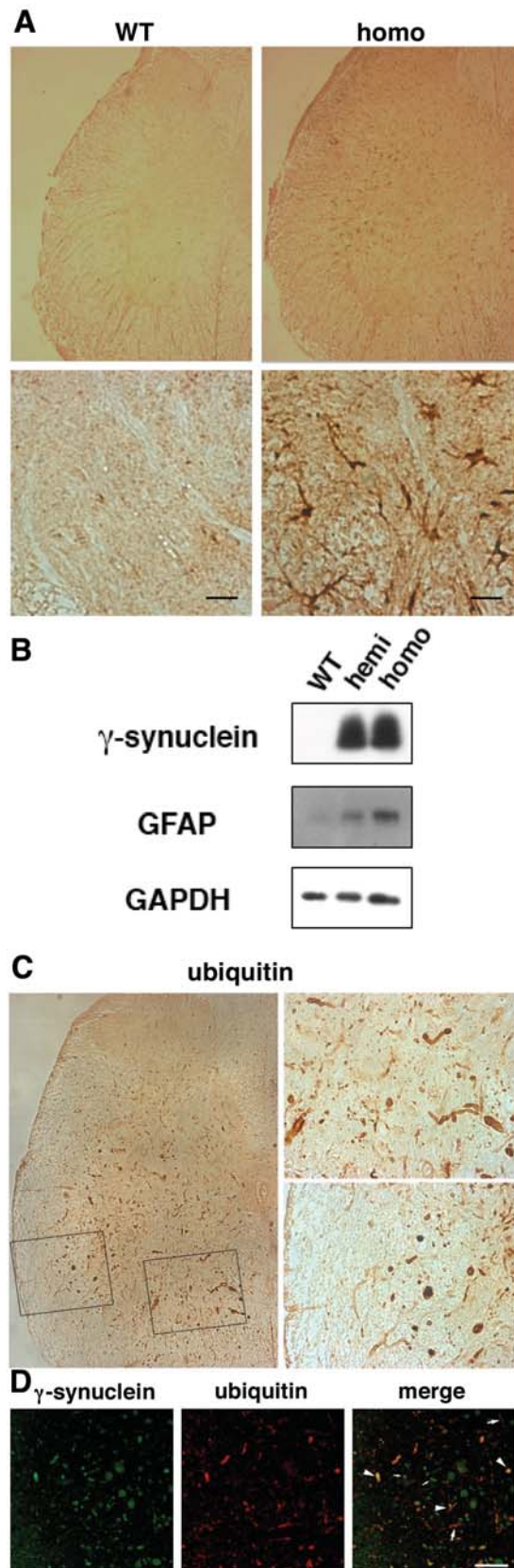


**Figure 5.** Amyloid deposits in the spinal cord of  $\gamma$ -synuclein transgenic mice. Representative images of Congo Red-stained spinal cord sections of 12-month-old wild-type mouse (A), hemizygous Thy1 $\mu$ γSN mouse (B), homozygous Thy1 $\mu$ γSN mouse at the advance stage of pathology (C) and homozygous Thy1 $\mu$ γSN mouse with mild signs of pathology (D) are shown. Scale bar = 200  $\mu$ m for all main panels and 25  $\mu$ m for all insets. The bar chart shows mean  $\pm$  SEM. of the number of deposits per randomly selected 0.1 mm<sup>2</sup> area of the spinal cord gray matter. Sections for counting [104 for (A), 121 for (B), 93 for (C) and 72 for (D)] were randomly selected throughout the length of cervical, thoracic and lumbar parts of the spinal cord of at least four animals per group. One-way ANOVA with *post hoc* Fisher's protected *t*-test demonstrated significant (\*\* $P < 0.01$ ) difference between all four experimental groups.



transgenic animals, we detected multiple abnormal ubiquitin-positive structures (Fig. 6C). However, double immunofluorescence revealed only partial overlap between  $\gamma$ -synuclein-positive and ubiquitin-positive profiles (Fig. 6D). Furthermore, western blot analysis did not reveal  $\gamma$ -synuclein-laddered staining patterns reminiscent of different degrees of ubiquitination (for example, see Fig. 1D). Therefore, most of the aggregated  $\gamma$ -synuclein in the spinal cord of Thy1 $\mu$  $\gamma$ SN mice are probably not ubiquitinated, but ubiquitin and/or some ubiquitinated proteins are present in the inclusions that appear in the nervous system of these mice.

#### Loss of motor neurons in the spinal cord of transgenic mice

The emergence of pathological inclusions and astrogliosis in Thy1 $\mu$  $\gamma$ SN mice coincides with the loss of motor neurons in the spinal cord (Fig. 7). Twelve-month-old homozygous animals with severe motor impairments possessed less than 40% of their wild-type littermates spinal motor neuron complement (Fig. 7E). Age-matched hemizygous and homozygous mice that developed milder motor impairment (claspings reflex and pareses of one limb but normal righting, for example see Supplementary Material movie) also displayed motor neuron loss but to a far lesser extent (Fig. 7E). Similar results were obtained in cervical, thoracic and lumbar parts of the spinal cord (data not shown).

Neurodegeneration in the spinal cord of motor neuron disease patients is often associated with dysfunction of intracellular systems that are responsible for correct folding of protein molecules. Survival of spinal motor neurons seems to rely on molecular chaperons including small heat shock proteins (40–44). Therefore, we used western blot analysis to examine the levels of large (HSP70) and small (HSPB1 also known as HSP27 or, in mouse, HSP25) heat shock proteins in the spinal cords of Thy1 $\mu$  $\gamma$ SN mice. While the levels of HSP70 were similar in age-matched transgenic and wild-type animals, the levels of HSPB1 were dramatically increased in all ageing transgenic animals and particularly in those that displayed severe motor impairment (Supplementary Material Fig. S3). However, this increase was due to high levels of HSPB1 in activated astrocytes (Fig. 7F and Supplementary Material Fig. S4), whereas in spinal motor neurons of transgenic animals the level of this protein was substantially lower than in spinal motor neurons of wild-type mice (Fig. 7F).

**Figure 6.** Astrogliosis and ubiquitin-positive inclusions in the spinal cord of  $\gamma$ -synuclein transgenic mice. (A) Transverse sections through the spinal cord of wild-type and severely affected homozygous Thy1 $\mu$  $\gamma$ SN mice immunostained for GFAP. Higher magnification images are shown on lower panels, scale bars = 20  $\mu$ m. (B) Western blot of total protein extracts from 12-month-old wild-type, hemizygous and homozygous transgenic mice probed with antibodies against  $\gamma$ -synuclein, GFAP and GAPDH as a loading control. (C) Transverse sections through the spinal cord of severely affected homozygous Thy1 $\mu$  $\gamma$ SN mouse immunostained for ubiquitin. Boxed areas of gray and white matter are shown at higher magnification on the right top and right bottom panels, correspondingly. (D) Double immunofluorescent staining of severely affected Thy1 $\mu$  $\gamma$ SN mouse spinal cord section with antibodies against ubiquitin (green) and  $\gamma$ -synuclein (red). Examples of dystrophic neuritis and spheroids positive only for  $\gamma$ -synuclein are marked with large arrows, positive only for ubiquitin—with small arrows and positive for both proteins—with arrowheads. Scale bar = 50  $\mu$ m.



## Neurofilaments in the spinal cord and peripheral nerves of transgenic mice

HSPB1 is thought to be involved in regulation of the neurofilament network assembly in normal motor neurons and its mutant variants affect neurofilament-L (NF-L) aggregation in certain forms of Charcot–Marie–Tooth disease (45–47). An acute overexpression of  $\gamma$ -synuclein in cultured neurons also perturbs their neurofilament network integrity (15). Therefore, we analysed neurofilaments in the spinal motor neurons of transgenic mice chronically overexpressing  $\gamma$ -synuclein. Western blot analysis of the non-ionic detergent soluble fraction of Thy1 $\gamma$ SN mouse spinal cord revealed not only monomeric full-length 67 kDa NF-L but also distinct lower molecular weight NF-L species (Fig. 8A), possibly products of specific and restricted breakdown that were not seen in similar fractions of wild-type mouse spinal cord tissue. Decrease of these truncated species in the spinal cord of severely affected animals probably reflects loss of neurons that produced them. Overexpressed  $\gamma$ -synuclein co-immunoprecipitated with soluble NF-L, although substantially less amount of this protein was pulled-down from spinal cord lysates of animals at the advance stages of pathology than from similar lysates of less-affected animals (Fig. 8B).

Immunostaining of histological sections with antibody against NF-L did not reveal accumulation of this protein in  $\gamma$ -synuclein-positive or any other pathological profiles in the spinal cord of transgenic animals (Fig. 8C). However, substantial reduction in staining intensity in the spinal cord of Thy1 $\gamma$ SN mice when compared with wild-type tissue was observed (Fig. 8C). This reduction was mainly confined to neuronal processes and not the motor neuron cell bodies (Fig. 8D, upper panels). It was even more obvious in longitudinal sections through peripheral nerves of Thy1 $\gamma$ SN mice where only thin and wavy neurofilament-positive strings were found (Fig. 8D, lower panels). In addition, severe axonal pathology in the form of multiple nerve fibre swellings was revealed in the sciatic nerve of ageing homozygous Thy1 $\gamma$ SN mice (Fig. 8D, lower panels). Similar changes were also observed in tissue sections stained with antibodies against two other neurofilament proteins (data not shown). These results suggest that overexpression of  $\gamma$ -synuclein in transgenic mouse neurons seriously compromises the organization of neurofilaments in neuronal processes and, consequently, the architecture and function of axons.

## DISCUSSION

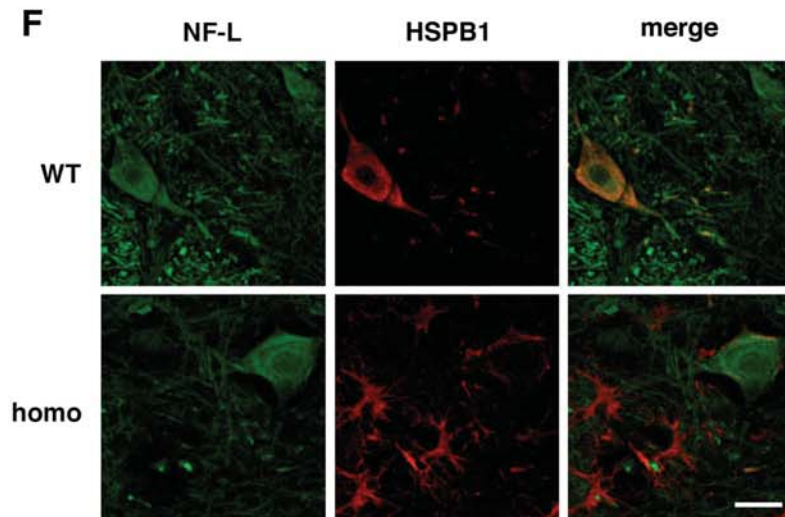
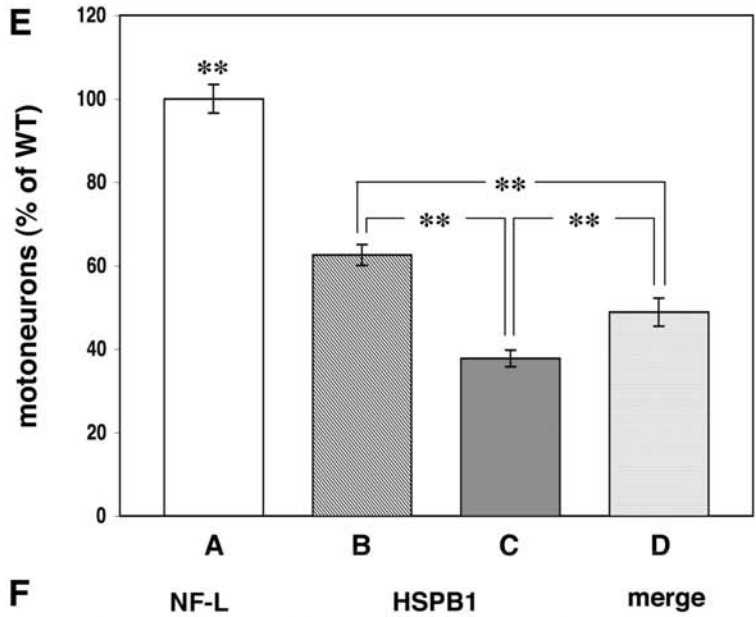
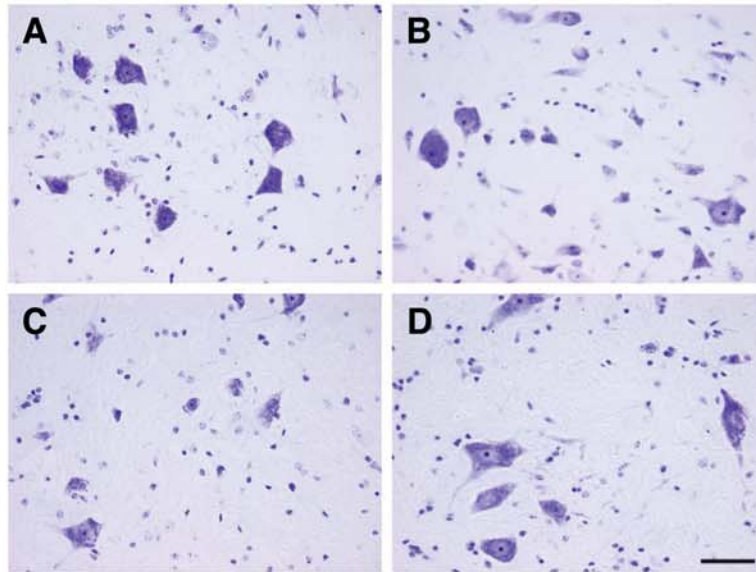
Previous studies of transgenic mice overexpressing members of the synuclein family have revealed the contrasting effects of  $\alpha$ -synuclein and  $\beta$ -synuclein on the development of pathological changes in the nervous system of these animals. High levels of  $\alpha$ -synuclein in neurons cause a prominent neurological phenotype although the manifestations are variable and dependent on the  $\alpha$ -synuclein isoform and type of promoter used for production of that particular transgenic line (reviewed in Refs. 48–50). In contrast, overexpression of  $\beta$ -synuclein does not have a harmful effect on animal health and even counteracts  $\alpha$ -synuclein neurotoxicity (5–7). These results echo differences in aggregation propensity, cytotoxicity and

certain structural features of these two proteins. As discussed in the Introduction,  $\gamma$ -synuclein has molecular features shared with both  $\alpha$ - and  $\beta$ -synuclein. Therefore, it was not possible to predict the consequences of  $\gamma$ -synuclein overexpression in the nervous system of transgenic animals. Revealing the effects of aberrant expression of  $\gamma$ -synuclein *in vivo* is important not only for better understanding of relationships between structure and function within synuclein family. This information would also be valuable for development of new therapeutic approaches to combat synucleinopathies.

No disease-associated mutations of  $\gamma$ -synuclein gene or obvious cases of idiopathic human  $\gamma$ -synucleinopathies have been reported so far and the amino acid similarity between human and mouse proteins is high. Taking these facts into consideration, we decided to create a simple homologous model in which mouse  $\gamma$ -synuclein was overexpressed in the majority of neurons of the mouse nervous system. To achieve this we produced Thy1 $\gamma$ SN transgenic mice, expressing high levels of mouse  $\gamma$ -synuclein under control of the Thy-1 promoter cassette that has previously been used for producing several  $\alpha$ -synuclein (27–30) and a  $\beta$ -synuclein (5) transgenic animal lines. In relatively homogeneous populations of neurons that normally express  $\gamma$ -synuclein, for example the DRG, there was approximately a 7-fold increase of  $\gamma$ -synuclein mRNA expression in homozygous Thy1 $\gamma$ SN transgenic mice compared with wild-type mice.

In homozygous transgenic mice,  $\gamma$ -synuclein aggregates and accumulates in abnormal structures within neuronal cell bodies and neurites. These  $\gamma$ -synuclein-positive structures resemble pathological hallmarks of synucleinopathies, namely dystrophic, beaded and ballooned neurites, spheroids, and even, occasionally, Lewy bodies. Like aggregated  $\alpha$ -synuclein, aggregated  $\gamma$ -synuclein could not be extracted from transgenic mouse neural tissues using non-ionic detergents, but is partially soluble in sarcosyl-containing buffers. At least a fraction of aggregated  $\gamma$ -synuclein forms linear fibrils that are structurally similar, although not identical to products of  $\alpha$ -synuclein fibrillation *in vivo* or *in vitro*.

Multimeric forms of  $\alpha$ -synuclein are commonly detected on western blots of SDS-soluble proteins extracted from neural tissues of patients suffered from synucleinopathies or  $\alpha$ -synuclein transgenic mice (35,37,38,51–55). These higher molecular weight bands represent either SDS-resistant  $\alpha$ -synuclein oligomers or ubiquitinated forms of the protein. We did not observe similar concatomeric  $\gamma$ -synuclein species in extracts of  $\gamma$ -synuclein transgenic mouse brain or spinal cord. This might suggest that the oligomeric intermediates of  $\gamma$ -synuclein aggregates are either not accumulating to a significant level in neurons of transgenic mice or that they are readily solubilized to monomeric  $\gamma$ -synuclein in SDS-containing buffers. It also suggests that even aggregated  $\gamma$ -synuclein is rarely ubiquitinated, which is consistent with our observation that  $\gamma$ -synuclein-positive inclusions in the spinal cord of transgenic mice often do not co-localize with ubiquitin-positive structures. The most probable explanation of our results is that ubiquitination is neither required for nor accompanies  $\gamma$ -synuclein aggregation but ubiquitin or certain ubiquitinated proteins may accumulate in pathological inclusions. Moreover, pathological changes in the nervous system of transgenic mice may trigger secondary events,



including aggregation of ubiquitinated proteins and formation of ubiquitin-positive/ $\gamma$ -synuclein-negative inclusions that we have observed on double-immunostained sections of the spinal cord. Similar partial overlap of  $\alpha$ -synuclein and ubiquitin staining patterns has been found previously in the nervous systems of patients with synucleinopathies and  $\alpha$ -synuclein transgenic mice, though ubiquitinated  $\alpha$ -synuclein is relatively abundant in these tissues (56).

The common features of  $\alpha$ -synuclein pathology in human patients and transgenic mice are abundant amyloid deposits and activated glial cells in affected areas of the nervous system. In the brain and spinal cord of  $\gamma$ -synuclein transgenic mice, we also observed multiple amyloid (Congo Red- and Thioflavin S-positive) deposits and prominent astrogliosis, but no activated microglia was detected.

Although all pathological changes described above were observed throughout the central nervous system of Thy1 $\gamma$ SN mice, the spinal cord was noticeably more affected than any other region, which is similar to the reports on transgenic mice expressing  $\alpha$ -synuclein under control of the same Thy-1 promoter (Refs 27,29,57 and our unpublished observations). This probably reflects the higher sensitivity of spinal cord neurons, particularly motor neurons, to high levels of both members of the synuclein family.

The ultimate consequence of  $\gamma$ -synuclein overexpression in transgenic mice is death of motor neurons. Correspondingly, these mice display clinical signs typical for motor neuron disease, namely a gradual development of motor deficit followed by pareses and paralyses, which are most obvious in limb muscles. At this terminal stage of the disease,  $\gamma$ -synuclein transgenic animals lose more than 60% of ventral horn motor neurons.

The development of neurological phenotype and histopathological findings in our mice suggests that pan-neuronal overexpression of  $\gamma$ -synuclein in mice could trigger pathological changes typical for synucleinopathies and most apparent in the spinal cord. The burden of pathology increases with age, which leads to a gradual loss of spinal motor neurons and the development of motor dysfunction. The onset, penetrance and degree of neuropathology directly correlate with the level of transgene expression because the hemizygous animals, which express 50% less transgenic  $\gamma$ -synuclein than the homozygous animals, develop clinical signs later in their life and show less pronounced histopathological changes in their nervous system.

One intriguing question is which molecular and cellular processes previously linked to the development of neurodegeneration become compromised in the nervous system of  $\gamma$ -synuclein transgenic mice? Recent studies on the mechanisms of neurodegeneration in humans and in various model organisms demonstrate that simultaneous dysfunction of several systems safeguarding cell homeostasis is required for the development

of a full-scale pathology. However, some types of neurons are particularly sensitive to dysfunction in certain intracellular systems. Pathogenesis of motor neuron diseases often involves disruption of neurofilament networks in motor neuron cell bodies and axons (reviewed in Refs 58–61). While this disruption could be triggered by various mechanisms, in the majority of cases changes in the structure or metabolism of NF-L, a subunit required for assembly of neurofilaments *in vivo*, play a crucial role (45,62–67). We have demonstrated that chronic overexpression of  $\gamma$ -synuclein in mouse motor neurons leads to substantial depletion of neurofilaments in neuronal processes. This might be an essential event in pathogenesis of axonal pathology in peripheral nerves and consequent development of motor dysfunction in  $\gamma$ -synuclein transgenic mice. This result is consistent with our previous findings that acute overexpression of  $\gamma$ -synuclein affects neurofilament network integrity in cultured neurons, particularly their axons (15). The exact mechanism of the disruptive effect of overexpressed  $\gamma$ -synuclein on neurofilaments remains to be elucidated but its ability to interact with soluble NF-L and accumulation of abnormal NF-L-reactive soluble polypeptides in the spinal cord of Thy1 $\gamma$ SN mice suggest that normal homeostasis, including transport of NF-L to axons, might be at least partially prevented by trapping this protein in complexes with  $\gamma$ -synuclein and/or abnormal degradation. Disruption of axonal neurofilaments follows the reduction of NF-L axonal traffic. Moreover, truncated NF-L species could also affect neurofilament assembly and/or stability.

Some histopathological changes observed in Thy1 $\gamma$ SN mice, including astrogliosis and loss of motor neurons and their axons, are similar to those observed in aged NF-L null mutant mice (67). However in  $\gamma$ -synuclein transgenic mice, the pathological phenotype develops much earlier and is substantially more severe. This suggests that, in addition to the disrupted neurofilament network, other intracellular systems are also compromised in the motor neurons of these animals. Molecular chaperons belonging to the family of heat shock proteins play an important protective role in motor neurons. These cells seem to be particularly vulnerable to dysfunction of the small heat shock protein HSPB1 (40–44) and mutations of the HSPB1 gene cause certain types of motor neuron diseases (45–47). In motor neurons of  $\gamma$ -synuclein transgenic mice, the level of HSP25, a mouse ortholog of HSPB1, is substantially reduced, potentially compromising the survival of these cells.

Although some  $\alpha$ -synuclein transgenic mice develop similar clinical signs of the spinal cord pathology to  $\gamma$ -synuclein transgenic mice, neither down-regulation of HSPB1 nor changes of the neurofilament network in their motor neurons has been reported. Taken together with other data, this suggests that diverse but partially overlapping mechanisms underlie development of pathology in these two mouse models.

**Figure 7.** Loss of motor neurons and changes of HSPB1 expression in the spinal cord of  $\gamma$ -synuclein transgenic mice. Representative images of cresyl fast violet-stained spinal cord sections of 12-month-old wild-type mouse (A), hemizygous Thy1 $\gamma$ SN mouse (B), homozygous Thy1 $\gamma$ SN mouse at the advance stage of pathology (C) and homozygous Thy1 $\gamma$ SN mouse with mild pathology (D) are shown. (E) The bar chart shows mean  $\pm$  SEM. of the number of motor neurons per section expressed as percent of the average number of motor neurons per section of the wild-type mouse spinal cord. Sections for counting [160 for (A), 332 for (B), 215 for (C) and 139 for (D)] were randomly selected throughout the length of cervical, thoracic and lumbar parts of the spinal cord of at least four animals per group. One-way ANOVA with *post hoc* Fisher's protected *t*-test demonstrated significant (\*\* $P < 0.01$ ) difference between all four experimental groups. (F) Double immunofluorescent staining of spinal cord sections from a wild-type mouse and severely affected homozygous Thy1 $\gamma$ SN mouse with antibodies against neurofilament-L (green) and HSPB1 (red). Scale bar = 20  $\mu$ m.

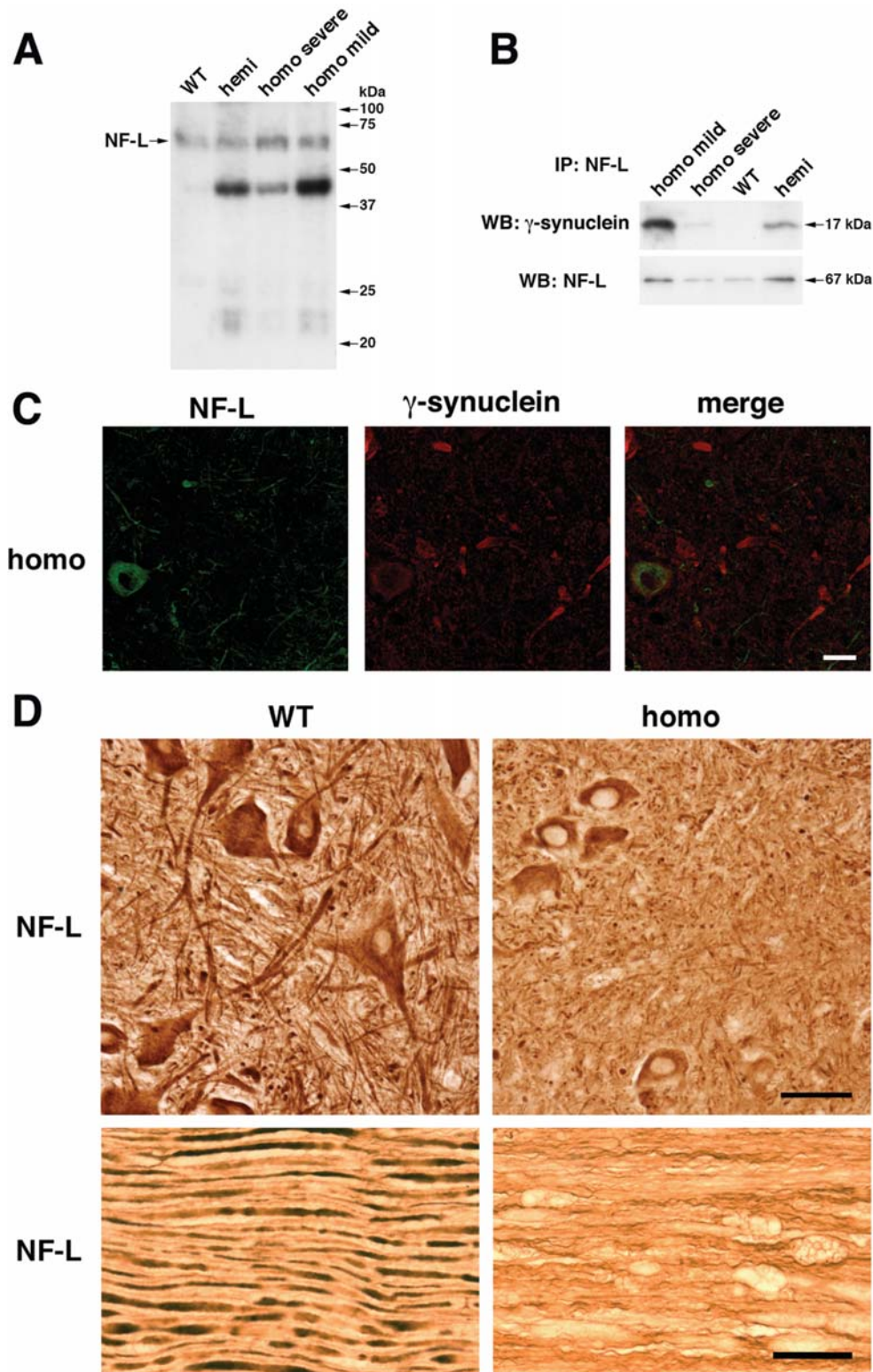


**Figure 8.** Neurofilaments in the spinal cord and peripheral nerve of  $\gamma$ -synuclein transgenic animals. **(A)** Western blot analysis of soluble neurofilament-L in the cytosolic (10 000g supernatant) fraction of the spinal cord of 12-month-old wild-type mice, hemizygous Thy1 $\gamma$ SN mice, homozygous Thy1 $\gamma$ SN mice with mild clinical signs of pathology and homozygous Thy1 $\gamma$ SN mice at the advance stage of pathology. **(B)** Co-immunoprecipitation of  $\gamma$ -synuclein and soluble neurofilament-L from the same cytosolic fractions. **(C)** Double immunofluorescent staining of severely affected Thy1 $\gamma$ SN mouse spinal cord section with antibodies against neurofilament-L (green) and  $\gamma$ -synuclein (red) shows the absence of NF-L accumulation in  $\gamma$ -synuclein-positive pathological profiles. **(D)** Substantial reduction of neurofilament-L staining in the ventral horns of the spinal cord (upper panels) and sciatic nerve (lower panels) of 12-month-old homozygous Thy1 $\gamma$ SN mice at the advance stage of pathology compared with their wild-type littermates. Scale bars = 20  $\mu$ m for (C) and 50  $\mu$ m for (D).

In conclusion, we have demonstrated that transgenic mice expressing high levels of  $\gamma$ -synuclein in their neurons develop a severe neurodegenerative pathology. It is feasible that, under certain conditions,  $\gamma$ -synuclein could be involved in the development of pathological changes in human neurons. Further studies on the role of this synuclein in normal and degenerating neurons might therefore provide additional insight into the mechanisms leading to human neurodegenerative diseases.

## MATERIALS AND METHODS

### Generation of transgenic animals

A fragment of mouse  $\gamma$ -synuclein cDNA including 34 bp of 5'-UTR and 64 bp of 3'-UTR was PCR amplified using pD53 plasmid DNA (31) as a template and oligonucleotides with *Xho*I linkers (m $\gamma$ SN *Xho*I-F: 5'-CTACTGTCCGCTCG AGCTTGACAGCCAGGTC-3' and m $\gamma$ SN *Xho*I-R: 5'-CTACTGTCCGCTCGAGGCCTTCTAGTCTTCTCCA-C-3') to facilitate subsequent cloning into *Xho*I site of Thy-1 promoter plasmid 323-pTSC21k (27). The fragment for microinjecting mouse oocytes was isolated by digestion of the resulting plasmid DNA with *Not*I. Transgenic founders were produced on C57Bl6 genetic background. Animals positive for transgene expression were crossed with C57Bl6 wild-type mice. Transgenic and wild-type animals were identified by PCR analysis of DNA from ear biopsies. The presence of a 1 kb product in the amplification reaction with primers HP45 *Thy*1 f2 (5'-ACACCCCTAAAGCATAACAGTCAGAC C-3') and HP84 m  $\gamma$ SN (5'-GGCCTTCTAGTCTTCTCCA CTCTTG-3') indicated the presence of transgene in the mouse genome. Experimental cohorts were formed from litters produced by intercrossing hemizygous animals. Hemi- and homozygous animals were discriminated by quantitative real-time PCR analysis of DNA from ear biopsies and verified by analytical backcrossing followed by offspring genotyping. All animal work was carried in accordance with the United Kingdom Animals (Scientific Procedures) Act (1986).

### Motor performance tests

**Rotarod tests.** Animals were tested on Ugo Basile 7650 rotarod at 2, 4, 6, 9, 12, 18 and 24 months of age. A constant (24 rpm) speed test was carried out for 4 min and accelerating (4–40 rpm) speed test for 5 min as described previously (68). Each mouse was tested three times in each mode with at least 30 min rest between trials. The mean of latency to fall for these three trials was included in final statistics. Eleven wild type, 12 hemizygous and 13 homozygous mice were tested at 2 months: 28, 27 and 21, at 4 months; 35, 40 and 23, at 6 months; 34, 36 and 23, at 9 months; 25, 26 and 14, at 12 months of age. No homozygous animals survived beyond 16 months therefore at this age and at 24 months only wild-type (12 and 15, respectively) and hemizygous (21 and 15, respectively) animals were tested.

**Horizontal beam test.** Animal coordination was tested on an 11 mm diameter and 50 cm long horizontal wooden rod at 4, 6, 9 and 12 months of age. A mouse was placed at the free

hanging end of the rod facing its end. The ability to turn 180° and to reach an escape black box at the other end of the rod was recorded.

**Footprint test.** Animals were trained to run along a narrow passage lined with a strip of white paper before carrying out the test run. For this run, mouse forefeet were coated with blue ink and hindfeet with red ink. Different parameters of the stride were measured and analysed as described previously (69).

### RNA expression analysis

Total RNA from various regions of the nervous system was extracted using RNeasy+ kit as recommended by the manufacturer (Qiagen). First-strand cDNA was synthesized using random primers (Promega) and SuperScriptIII reverse transcriptase (Invitrogen). Quantitative PCR was performed on StepOne Real-Time PCR System (Applied Biosystems) with DyNAmo HS SYBR Green supermix (Finnzymes) and ROX as a passive reference dye. Reactions were carried out in one-piece thin-wall 48-well PCR plates (Bioplastics). GAPDH mRNA was used as a normalization standard. Primers 5'-CCATGGACGTCTTCAAGAAAGG-3' and 5'-CGTTCTC CTTGGTTTTGGTG-3' were used for amplification of  $\gamma$ -synuclein cDNA, and primers 5'-CACTGAGCATCTCC CTCACA-3' and 5'-GTGGGTGCAGCGAACTTTAT-3' for amplification of GAPDH mRNA. After hot start (10 min at 95°C), 40 cycles of 15 s at 95°C and 60 s at 60°C were carried out followed by melting curve determination with 0.3°C steps. Fold change was determined by  $2^{-\Delta\Delta CT}$  method as described previously (70) using StepOne v2.0 software.

### Protein extraction

Total tissue proteins were extracted by homogenization of tissues directly in SDS-PAGE loading buffer followed by incubation for 10 min at 100°C. For analysis of cytosolic proteins, tissues were homogenized in 50 mM Tris-HCl, pH 7.5; 150 mM NaCl; 1% Triton X-100 buffer with protease inhibitors (Complete Mini from Roche) and cytosolic fraction was obtained by centrifugation for 10 min at 10 000g.

### Sequential protein extraction

A previously described protocol (37) was used with minor modifications. Briefly, neuronal tissues were homogenized in 5 volumes of high salt (HS) buffer (50 mM Tris-HCl, pH 7.5; 750 mM NaCl; 5 mM EDTA) with protease inhibitors (Complete Mini from Roche) and centrifuged at 100 000g for 20 min at 4°C. Pellets were washed in the same buffer and then re-extracted in HS buffer containing 1% Triton X-100 (HS/T-soluble fraction). Subsequent centrifugations and re-extractions produced RIPA-soluble and SDS-soluble fractions. The presence of  $\gamma$ -synuclein in these fractions was analysed by SDS-PAGE/western blotting.

### Isolation and visualization of $\gamma$ -synuclein filaments

Sarcosyl-insoluble filaments were extracted from mouse spinal cords as described previously for human neuronal tissues (71).

Final 100 000g pellets were resuspended in 50 mM Tris–HCl (pH 7.5) buffer and aliquots were applied onto glow-discharged carbon-coated 400-mesh copper grids. After blocking in 1% BSA/PBS, grids were incubated in 1:50 diluted affinity purified rabbit anti-mouse  $\gamma$ -synuclein SK23 antibody (31) for 60 min at room temperature followed by goat anti-rabbit immunoglobulin secondary antibody (Amersham) conjugated to 10 nm gold particles. Fibrils were negatively stained with 1% dodeca-tungstophosphoric acid neutralized with KOH to pH 6.2 as described previously (72) and observed at  $\times 40\,000$  or  $\times 50\,000$  magnification under a Philips TEM 208 transmission electron microscope.

### Western blotting and antibodies

Proteins separated by SDS–PAGE were transferred to PVDF membrane using iBlot technology according to manufacturer (Invitrogen) instructions. Membrane blocking, incubation with antibodies, washing and chemiluminescent detection using ECL or ECL<sup>+</sup> techniques were carried out as described previously (31,68). Intensities of bands obtained using AlphaImager 2200 were analysed using AlphaEase 2200 Analysis Software (AlphaInnotech Corporation). Primary antibodies against GAPDH (mouse monoclonal, clone 6C5, Santa Cruz Biotechnology),  $\alpha$ -synuclein (mouse monoclonal, clone 42, BD Transduction Laboratories),  $\beta$ -synuclein (mouse monoclonal, clone 8, BD Transduction Laboratories),  $\gamma$ -synuclein (rabbit polyclonal SK23, affinity purified), GFAP (rabbit polyclonal, Sigma), Iba1 (mouse monoclonal, clone 1022-5, Santa Cruz), CD11b (rat monoclonal, clone M1/70.15, Serotec), NF-L (rabbit monoclonal, clone C28E10, and mouse monoclonal, clone DA2, both Cell Signalling), neurofilament H (rabbit polyclonal, Sigma), heat shock protein B1 (rabbit monoclonal, Cell Signalling) and heat shock protein 70 (rabbit monoclonal, Cell Signalling) were used.

### Immunoprecipitation

Freshly dissected spinal cords from individual animals were homogenized in 0.5 ml of IP buffer (50 mM Tris–HCl, pH 7.5, 300 mM NaCl, 1.5 mM MgCl<sub>2</sub>, 1% Triton X-100) with protease inhibitors (Complete Mini from Roche) and Triton-soluble fraction was obtained by  $\times 10\,000g$  centrifugation for 10 min at 4°C. After presorption on Protein G Sepharose (Amersham) for 30 min at 4°C and removal of beads by centrifugation for 1 min at 1000g, 5  $\mu$ l of antibody against NF-L (mouse monoclonal, clone DA2, Cell Signalling) or 20  $\mu$ l of antibody against  $\gamma$ -synuclein (rabbit polyclonal SK23) were added, followed by 50  $\mu$ l of fresh Protein G Sepharose. The suspension was rotated at 4°C for 2 h Sepharose beads were collected by centrifugation for 1 min at 1000g and washed four times with IP buffer. Bound proteins were eluted by boiling beads in 50  $\mu$ l of SDS–PAGE loading buffer for 10 min.

### Histological techniques

Dissected tissues were post-fixed in 4% paraformaldehyde/PBS or Carnoy's fixative and embedded in paraffin wax. Eight micrometre thick sections were cut and immunostained

as described previously (32) using Elite plus kits (Vector laboratories) and 3,3'-diaminobenzidine as a substrate. For double immunofluorescence, secondary Alexa Fluor-conjugated antibody (Invitrogen) were used. Images were prepared using laser scanning confocal microscope Leica TCS SP2 (Leica Microsystems) and LEICA CONFOCAL 2.00 software. For detection and counting of amyloid aggregates, spinal cord sections (four to five animals per age/genotype/condition group) were stained in 0.5% Congo red solution in 50% ethanol for 7 min followed by a brief differentiation in potassium hydroxide (0.2% in 80% ethanol) and, after several washes in dH<sub>2</sub>O, were mounted using Immu-mount (Thermo Electron Corporation). Fluorescent microscopy was used to analyse the number of aggregates within a randomly selected 0.1 mm<sup>2</sup> area of the spinal cord gray matter. For assessing number of spinal motor neurons, transverse spinal cord sections were stained in 0.5% cresyl fast violet (CFV) solution in dH<sub>2</sub>O and dissociated in acidified ethanol (0.25% acetic acid in ethanol). The number of motor neurons (identified by a large cell body containing Nissl granules, with a clear nuclear envelope containing a strongly stained nucleolus) within the ventral horn was counted. Results were expressed as per cent of the average number of motor neurons per ventral horn section in the wild-type animals.

### SUPPLEMENTARY MATERIAL

Supplementary Material is available at *HMG* online.

### ACKNOWLEDGEMENTS

We are grateful to K.H. Wiederhold, Simone Danner, Sabine Kauffmann, Chiara Mencarelli, Abdelmojib Al-Wandi and Robert Durkin for preliminary analysis done at an early stage of this project; Matthias Mueller and Bernd Kinzel for help in generating the transgenic lines; Anthony Hann and Simon Brooks for valuable advices and Rosalind John for critical reading of the manuscript.

*Conflict of Interest statement.* None declared.

### FUNDING

This work was supported by The Wellcome Trust [grant number 075615]. Funding to pay the Open Access publication charges for this article was provided by The Wellcome Trust.

### REFERENCES

1. Cookson, M.R. and van der Brug, M. (2008) Cell systems and the toxic mechanism(s) of alpha-synuclein. *Exp. Neurol.*, **209**, 5–11.
2. Park, J.Y. and Lansbury, P.T. Jr (2003) Beta-synuclein inhibits formation of alpha-synuclein protofibrils: a possible therapeutic strategy against Parkinson's disease. *Biochemistry*, **42**, 3696–3700.
3. da Costa, C.A., Masliah, E. and Checler, F. (2003) Beta-synuclein displays an antiapoptotic p53-dependent phenotype and protects neurons from 6-hydroxydopamine-induced caspase 3 activation: cross-talk with alpha-synuclein and implication for Parkinson's disease. *J. Biol. Chem.*, **278**, 37330–37335.
4. Windisch, M., Hutter-Paier, B., Rockenstein, E., Hashimoto, M., Mallory, M. and Masliah, E. (2002) Development of a new treatment for

- Alzheimer's disease and Parkinson's disease using anti-aggregatory beta-synuclein-derived peptides. *J. Mol. Neurosci.*, **19**, 63–69.
5. Hashimoto, M., Rockenstein, E., Mante, M., Mallory, M. and Masliah, E. (2001)  $\beta$ -Synuclein inhibits alpha-synuclein aggregation: a possible role as an anti-parkinsonian factor. *Neuron*, **32**, 213–223.
  6. Fan, Y., Limprasert, P., Murray, I.V., Smith, A.C., Lee, V.M., Trojanowski, J.Q., Sopher, B.L. and La Spada, A.R. (2006) Beta-synuclein modulates alpha-synuclein neurotoxicity by reducing alpha-synuclein protein expression. *Hum. Mol. Genet.*, **15**, 3002–3011.
  7. Hashimoto, M., Rockenstein, E., Mante, M., Crews, L., Bar-On, P., Gage, F.H., Marr, R. and Masliah, E. (2004) An antiaggregation gene therapy strategy for Lewy body disease utilizing beta-synuclein lentivirus in a transgenic model. *Gene Ther.*, **11**, 1713–1723.
  8. Sung, Y.H. and Eliezer, D. (2007) Residual structure, backbone dynamics, and interactions within the synuclein family. *J. Mol. Biol.*, **372**, 689–707.
  9. Volles, M.J. and Lansbury, P.T. Jr (2003) Zeroing in on the pathogenic form of alpha-synuclein and its mechanism of neurotoxicity in Parkinson's disease. *Biochemistry*, **42**, 7871–7878.
  10. Dev, K.K., Hofele, K., Barbieri, S., Buchman, V.L. and van der Putten, H. (2003) Part II: alpha-synuclein and its molecular pathophysiological role in neurodegenerative disease. *Neuropharmacology*, **45**, 14–44.
  11. Biere, A.L., Wood, S.J., Wypych, J., Steavenson, S., Jiang, Y., Anafi, D., Jacobsen, F.W., Jarosinski, M.A., Wu, G.M., Louis, J.C. *et al.* (2000) Parkinson's disease-associated alpha-synuclein is more fibrillogenic than beta- and gamma-synuclein and cannot cross-seed its homologs. *J. Biol. Chem.*, **275**, 34574–34579.
  12. Uversky, V.N., Li, J., Souillac, P., Millett, I.S., Doniach, S., Jakes, R., Goedert, M. and Fink, A.L. (2002) Biophysical properties of the synucleins and their propensities to fibrillate: inhibition of alpha-synuclein assembly by beta- and gamma-synucleins. *J. Biol. Chem.*, **277**, 11970–11978.
  13. Zibace, S., Jakes, R., Fraser, G., Serpell, L.C., Crowther, R.A. and Goedert, M. (2007) Sequence determinants for amyloid fibrillogenesis of human alpha-synuclein. *J. Mol. Biol.*, **374**, 454–464.
  14. Saha, A.R., Ninkina, N.N., Hanger, D.P., Anderton, B.H., Davies, A.M. and Buchman, V.L. (2000) Induction of neuronal death by alpha-synuclein. *Eur. J. Neurosci.*, **12**, 3073–3077.
  15. Buchman, V.L., Adu, J., Pinon, L.G., Ninkina, N.N. and Davies, A.M. (1998) Persyn, a member of the synuclein family, influences neurofilament network integrity. *Nat. Neurosci.*, **1**, 101–103.
  16. Surgucheva, I., McMahan, B., Ahmed, F., Tomarev, S., Wax, M.B. and Surguchov, A. (2002) Synucleins in glaucoma: implication of gamma-synuclein in glaucomatous alterations in the optic nerve. *J. Neurosci. Res.*, **68**, 97–106.
  17. Rockenstein, E., Hansen, L.A., Mallory, M., Trojanowski, J.Q., Galasko, D. and Masliah, E. (2001) Altered expression of the synuclein family mRNA in Lewy body and Alzheimer's disease. *Brain Res.*, **914**, 48–56.
  18. Mukaetova-Ladinska, E.B., Milne, J., Andras, A., Abdel-All, Z., Cerejeira, J., Grealley, E., Robson, J., Jaros, E., Perry, R., McKeith, I.G. *et al.* (2008) Alpha- and gamma-synuclein proteins are present in cerebrospinal fluid and are increased in aged subjects with neurodegenerative and vascular changes. *Dement. Geriatr. Cogn. Disord.*, **26**, 32–42.
  19. Mori, F., Hayashi, S., Yamagishi, S., Yoshimoto, M., Yagihashi, S., Takahashi, H. and Wakabayashi, K. (2002) Pick's disease: alpha- and beta-synuclein-immunoreactive Pick bodies in the dentate gyrus. *Acta Neuropathol. (Berl.)*, **104**, 455–461.
  20. Galvin, J.E., Giasson, B., Hurtig, H.I., Lee, V.M. and Trojanowski, J.Q. (2000) Neurodegeneration with brain iron accumulation, type 1 is characterized by alpha-, beta-, and gamma-synuclein neuropathology. *Am. J. Pathol.*, **157**, 361–368.
  21. Galvin, J.E., Uryu, K., Lee, V.M. and Trojanowski, J.Q. (1999) Axon pathology in Parkinson's disease and Lewy body dementia hippocampus contains alpha-, beta-, and gamma-synuclein. *Proc. Natl Acad. Sci. USA*, **96**, 13450–13455.
  22. Mu, X., Beremand, P.D., Zhao, S., Pershad, R., Sun, H., Scarpa, A., Liang, S., Thomas, T.L. and Klein, W.H. (2004) Discrete gene sets depend on POU domain transcription factor Brn3b/Brn-3.2/POU4f2 for their expression in the mouse embryonic retina. *Development*, **131**, 1197–1210.
  23. Brenz Verca, M.S., Bahi, A., Boyer, F., Wagner, G.C. and Dreyer, J.L. (2003) Distribution of alpha- and gamma-synucleins in the adult rat brain and their modification by high-dose cocaine treatment. *Eur. J. Neurosci.*, **18**, 1923–1938.
  24. Soto, I., Oglesby, E., Buckingham, B.P., Son, J.L., Roberson, E.D., Steele, M.R., Inman, D.M., Vetter, M.L., Horner, P.J. and Marsh-Armstrong, N. (2008) Retinal ganglion cells downregulate gene expression and lose their axons within the optic nerve head in a mouse glaucoma model. *J. Neurosci.*, **28**, 548–561.
  25. Buckingham, B.P., Inman, D.M., Lambert, W., Oglesby, E., Calkins, D.J., Steele, M.R., Vetter, M.L., Marsh-Armstrong, N. and Horner, P.J. (2008) Progressive ganglion cell degeneration precedes neuronal loss in a mouse model of glaucoma. *J. Neurosci.*, **28**, 2735–2744.
  26. Wang, Y.L., Takeda, A., Osaka, H., Hara, Y., Furuta, A., Setsuie, R., Sun, Y.J., Kwon, J., Sato, Y., Sakurai, M. *et al.* (2004) Accumulation of beta- and gamma-synucleins in the ubiquitin carboxyl-terminal hydrolase L1-deficient gad mouse. *Brain Res.*, **1019**, 1–9.
  27. van der Putten, H., Wiederhold, K.H., Probst, A., Barbieri, S., Mistl, C., Danner, S., Kauffmann, S., Hofele, K., Spooen, W.P., Ruegg, M.A. *et al.* (2000) Neuropathology in mice expressing human alpha-synuclein. *J. Neurosci.*, **20**, 6021–6029.
  28. Rockenstein, E., Mallory, M., Hashimoto, M., Song, D., Shults, C.W., Lang, I. and Masliah, E. (2002) Differential neuropathological alterations in transgenic mice expressing alpha-synuclein from the platelet-derived growth factor and Thy-1 promoters. *J. Neurosci. Res.*, **68**, 568–578.
  29. Chandra, S., Gallardo, G., Fernandez-Chacon, R., Schluter, O.M. and Sudhof, T.C. (2005) Alpha-synuclein cooperates with CSPalpha in preventing neurodegeneration. *Cell*, **123**, 383–396.
  30. Zhou, W., Schutzman, J. and Freed, C.R. (2008) Transgenic mice overexpressing tyrosine-to-cysteine mutant human alpha-synuclein: a progressive neurodegenerative model of diffuse Lewy body disease. *J. Biol. Chem.*, **283**, 9863–9870.
  31. Buchman, V.L., Hunter, H.J., Pinon, L.G., Thompson, J., Privalova, E.M., Ninkina, N.N. and Davies, A.M. (1998) Persyn, a member of the synuclein family, has a distinct pattern of expression in the developing nervous system. *J. Neurosci.*, **18**, 9335–9341.
  32. Ninkina, N., Papachroni, K., Robertson, D.C., Schmidt, O., Delaney, L., O'Neill, F., Court, F., Rosenthal, A., Fleetwood-Walker, S.M., Davies, A.M. *et al.* (2003) Neurons expressing the highest levels of gamma-synuclein are unaffected by targeted inactivation of the gene. *Mol. Cell. Biol.*, **23**, 8233–8245.
  33. Yavich, L., Oksman, M., Tanila, H., Kerokoski, P., Hiltunen, M., van Groen, T., Puolivali, J., Mannisto, P.T., Garcia-Horsman, A., MacDonald, E. *et al.* (2005) Locomotor activity and evoked dopamine release are reduced in mice overexpressing A30P-mutated human alpha-synuclein. *Neurobiol. Dis.*, **20**, 303–313.
  34. Masliah, E., Rockenstein, E., Veinbergs, I., Mallory, M., Hashimoto, M., Takeda, A., Sagara, Y., Sisk, A. and Mucke, L. (2000) Dopaminergic loss and inclusion body formation in alpha-synuclein mice: implications for neurodegenerative disorders. *Science*, **287**, 1265–1269.
  35. Lee, M.K., Stirling, W., Xu, Y., Xu, X., Qui, D., Mandir, A.S., Dawson, T.M., Copeland, N.G., Jenkins, N.A. and Price, D.L. (2002) Human alpha-synuclein-harboring familial Parkinson's disease-linked Ala-53  $\rightarrow$  Thr mutation causes neurodegenerative disease with alpha-synuclein aggregation in transgenic mice. *Proc. Natl Acad. Sci. USA*, **99**, 8968–8973.
  36. Gispert, S., Del Turco, D., Garrett, L., Chen, A., Bernard, D.J., Hamm-Clement, J., Korf, H.W., Deller, T., Braak, H., Auburger, G. *et al.* (2003) Transgenic mice expressing mutant A53T human alpha-synuclein show neuronal dysfunction in the absence of aggregate formation. *Mol. Cell. Neurosci.*, **24**, 419–429.
  37. Giasson, B.I., Duda, J.E., Quinn, S.M., Zhang, B., Trojanowski, J.Q. and Lee, V.M. (2002) Neuronal alpha-synucleinopathy with severe movement disorder in mice expressing A53T human alpha-synuclein. *Neuron*, **34**, 521–533.
  38. Freichel, C., Neumann, M., Ballard, T., Muller, V., Woolley, M., Ozmen, L., Borroni, E., Kretschmar, H.A., Haass, C., Spooen, W. *et al.* (2007) Age-dependent cognitive decline and amygdala pathology in alpha-synuclein transgenic mice. *Neurobiol. Aging*, **28**, 1421–1435.
  39. Fleming, S.M., Salcedo, J., Fernagut, P.O., Rockenstein, E., Masliah, E., Levine, M.S. and Chesselet, M.F. (2004) Early and progressive sensorimotor anomalies in mice overexpressing wild-type human alpha-synuclein. *J. Neurosci.*, **24**, 9434–9440.
  40. Sharp, P.S., Akbar, M.T., Bouri, S., Senda, A., Joshi, K., Chen, H.J., Latchman, D.S., Wells, D.J. and de Bellerocche, J. (2008) Protective

- effects of heat shock protein 27 in a model of ALS occur in the early stages of disease progression. *Neurobiol. Dis.*, **30**, 42–55.
41. Maatkamp, A., Vlug, A., Haasdijk, E., Troost, D., French, P.J. and Jaarsma, D. (2004) Decrease of Hsp25 protein expression precedes degeneration of motoneurons in ALS-SOD1 mice. *Eur. J. Neurosci.*, **20**, 14–28.
  42. Bruening, W., Roy, J., Giasson, B., Figlewicz, D.A., Mushynski, W.E. and Durham, H.D. (1999) Up-regulation of protein chaperones preserves viability of cells expressing toxic Cu/Zn-superoxide dismutase mutants associated with amyotrophic lateral sclerosis. *J. Neurochem.*, **72**, 693–699.
  43. Adachi, H., Waza, M., Tokui, K., Katsuno, M., Minamiyama, M., Tanaka, F., Doyu, M. and Sobue, G. (2007) CHIP overexpression reduces mutant androgen receptor protein and ameliorates phenotypes of the spinal and bulbar muscular atrophy transgenic mouse model. *J. Neurosci.*, **27**, 5115–5126.
  44. Adachi, H., Katsuno, M., Minamiyama, M., Sang, C., Pagoulatos, G., Angelidis, C., Kusakabe, M., Yoshiki, A., Kobayashi, Y., Doyu, M. *et al.* (2003) Heat shock protein 70 chaperone overexpression ameliorates phenotypes of the spinal and bulbar muscular atrophy transgenic mouse model by reducing nuclear-localized mutant androgen receptor protein. *J. Neurosci.*, **23**, 2203–2211.
  45. Zhai, J., Lin, H., Julien, J.P. and Schlaepfer, W.W. (2007) Disruption of neurofilament network with aggregation of light neurofilament protein: a common pathway leading to motor neuron degeneration due to Charcot–Marie–Tooth disease-linked mutations in NFL and HSPB1. *Hum. Mol. Genet.*, **16**, 3103–3116.
  46. Evgrafov, O.V., Mersivanova, I., Irobi, J., Van Den Bosch, L., Dierick, I., Leung, C.L., Schagina, O., Verpoorten, N., Van Impe, K., Fedotov, V. *et al.* (2004) Mutant small heat-shock protein 27 causes axonal Charcot–Marie–Tooth disease and distal hereditary motor neuropathy. *Nat. Genet.*, **36**, 602–606.
  47. Ackerley, S., James, P.A., Kalli, A., French, S., Davies, K.E. and Talbot, K. (2006) A mutation in the small heat-shock protein HSPB1 leading to distal hereditary motor neuropathy disrupts neurofilament assembly and the axonal transport of specific cellular cargoes. *Hum. Mol. Genet.*, **15**, 347–354.
  48. Springer, W. and Kahle, P.J. (2006) Mechanisms and models of alpha-synuclein-related neurodegeneration. *Curr. Neurol. Neurosci. Rep.*, **6**, 432–436.
  49. Chesselet, M.F. (2008) In vivo alpha-synuclein overexpression in rodents: a useful model of Parkinson's disease? *Exp. Neurol.*, **209**, 22–27.
  50. Buchman, V.L. and Ninkina, N. (2008) Modulation of alpha-synuclein expression in transgenic animals for modelling synucleinopathies—is the juice worth the squeeze? *Neurotox. Res.*, **14**, 329–341.
  51. Yazawa, I., Giasson, B.I., Sasaki, R., Zhang, B., Joyce, S., Uryu, K., Trojanowski, J.Q. and Lee, V.M. (2005) Mouse model of multiple system atrophy alpha-synuclein expression in oligodendrocytes causes glial and neuronal degeneration. *Neuron*, **45**, 847–859.
  52. Masliah, E., Rockenstein, E., Veinbergs, I., Sagara, Y., Mallory, M., Hashimoto, M. and Mucke, L. (2001) Beta-amyloid peptides enhance alpha-synuclein accumulation and neuronal deficits in a transgenic mouse model linking Alzheimer's disease and Parkinson's disease. *Proc. Natl Acad. Sci. USA*, **98**, 12245–12250.
  53. Klucken, J., Shin, Y., Masliah, E., Hyman, B.T. and McLean, P.J. (2004) Hsp70 reduces alpha-synuclein aggregation and toxicity. *J. Biol. Chem.*, **279**, 25497–25502.
  54. Kahle, P.J., Neumann, M., Ozmen, L., Muller, V., Odoy, S., Okamoto, N., Jacobsen, H., Iwatsubo, T., Trojanowski, J.Q., Takahashi, H. *et al.* (2001) Selective insolubility of alpha-synuclein in human Lewy body diseases is recapitulated in a transgenic mouse model. *Am. J. Pathol.*, **159**, 2215–2225.
  55. Gomez-Isla, T., Irizarry, M.C., Mariash, A., Cheung, B., Soto, O., Schrupp, S., Söndel, J., Kotilinek, L., Day, J., Schwarzschild, M.A. *et al.* (2003) Motor dysfunction and gliosis with preserved dopaminergic markers in human alpha-synuclein A30P transgenic mice. *Neurobiol. Aging*, **24**, 245–258.
  56. Sampathu, D.M., Giasson, B.I., Pawlyk, A.C., Trojanowski, J.Q. and Lee, V.M. (2003) Ubiquitination of alpha-synuclein is not required for formation of pathological inclusions in alpha-synucleinopathies. *Am. J. Pathol.*, **163**, 91–100.
  57. Neumann, M., Kahle, P.J., Giasson, B.I., Ozmen, L., Borroni, E., Spooen, W., Muller, V., Odoy, S., Fujiwara, H., Hasegawa, M. *et al.* (2002) Misfolded proteinase K-resistant hyperphosphorylated alpha-synuclein in aged transgenic mice with locomotor deterioration and in human alpha-synucleinopathies. *J. Clin. Invest.*, **110**, 1429–1439.
  58. Xiao, S., McLean, J. and Robertson, J. (2006) Neuronal intermediate filaments and ALS: a new look at an old question. *Biochim. Biophys. Acta*, **1762**, 1001–1012.
  59. Lariviere, R.C. and Julien, J.P. (2004) Functions of intermediate filaments in neuronal development and disease. *J. Neurobiol.*, **58**, 131–148.
  60. Julien, J.P. and Kriz, J. (2006) Transgenic mouse models of amyotrophic lateral sclerosis. *Biochim. Biophys. Acta*, **1762**, 1013–1024.
  61. Bruijn, L.I., Miller, T.M. and Cleveland, D.W. (2004) Unraveling the mechanisms involved in motor neuron degeneration in ALS. *Annu. Rev. Neurosci.*, **27**, 723–749.
  62. Perez-Olle, R., Leung, C.L. and Liem, R.K. (2002) Effects of Charcot–Marie–Tooth-linked mutations of the neurofilament light subunit on intermediate filament formation. *J. Cell Sci.*, **115**, 4937–4946.
  63. Perez-Olle, R., Jones, S.T. and Liem, R.K. (2004) Phenotypic analysis of neurofilament light gene mutations linked to Charcot–Marie–Tooth disease in cell culture models. *Hum. Mol. Genet.*, **13**, 2207–2220.
  64. Mersivanova, I.V., Perepelov, A.V., Polyakov, A.V., Sitnikov, V.F., Dadali, E.L., Oparin, R.B., Petrin, A.N. and Evgrafov, O.V. (2000) A new variant of Charcot–Marie–Tooth disease type 2 is probably the result of a mutation in the neurofilament-light gene. *Am. J. Hum. Genet.*, **67**, 37–46.
  65. De Jonghe, P., Mersivanova, I., Nelis, E., Del Favero, J., Martin, J.J., Van Broeckhoven, C., Evgrafov, O. and Timmerman, V. (2001) Further evidence that neurofilament light chain gene mutations can cause Charcot–Marie–Tooth disease type 2E. *Ann. Neurol.*, **49**, 245–249.
  66. Beaulieu, J.M., Jacomy, H. and Julien, J.P. (2000) Formation of intermediate filament protein aggregates with disparate effects in two transgenic mouse models lacking the neurofilament light subunit. *J. Neurosci.*, **20**, 5321–5328.
  67. McLean, J.R., Sanelli, T.R., Leystra-Lantz, C., He, B.P. and Strong, M.J. (2005) Temporal profiles of neuronal degeneration, glial proliferation, and cell death in hNFL(+/+) and NFL(-/-) mice. *Glia*, **52**, 59–69.
  68. Robertson, D.C., Schmidt, O., Ninkina, N., Jones, P.A., Sharkey, J. and Buchman, V.L. (2004) Developmental loss and resistance to MPTP toxicity of dopaminergic neurons in substantia nigra pars compacta of gamma-synuclein, alpha-synuclein and double alpha/gamma-synuclein null mutant mice. *J. Neurochem.*, **89**, 1126–1136.
  69. Carter, R.J., Lione, L.A., Humby, T., Mangiarini, L., Mahal, A., Bates, G.P., Dunnett, S.B. and Morton, A.J. (1999) Characterization of progressive motor deficits in mice transgenic for the human Huntington's disease mutation. *J. Neurosci.*, **19**, 3248–3257.
  70. Livak, K.J. and Schmittgen, T.D. (2001) Analysis of relative gene expression data using real-time quantitative PCR and the 2(-Delta Delta C(T)) method. *Methods*, **25**, 402–408.
  71. Spillantini, M.G., Crowther, R.A., Jakes, R., Hasegawa, M. and Goedert, M. (1998) Alpha-synuclein in filamentous inclusions of Lewy bodies from Parkinson's disease and dementia with Lewy bodies. *Proc. Natl Acad. Sci. USA*, **95**, 6469–6473.
  72. Serpell, L.C., Berriman, J., Jakes, R., Goedert, M. and Crowther, R.A. (2000) Fiber diffraction of synthetic alpha-synuclein filaments shows amyloid-like cross-beta conformation. *Proc. Natl Acad. Sci. USA*, **97**, 4897–4902.